A Signal Decomposition Approach to Morphological Modeling of P wave

Ebadollah Kheirati Roonizi[1], Roberto Sassi[1]
[1] Dipartimento di Tecnologie dell'Informazione, Università degli Studi di Milano, Italy

Abstract

Morphological modelling of electrocardiographical P-waves could simplify the detection of signals' morphological features employed in risk stratification. We compared four different approaches, based on signal decomposition, for morphological modeling of signal-averaged P waves. The functional models included: trigonometric, Bézier, B-spline, and Gaussian basis functions.

The comparison between models was performed at a common fixed number of parameters (ranging between C=3 to 21). The performances of the approximations were evaluated using compression efficiency measures, like the percentage of root-mean-square differences (PRD). Non-linear iterative parameter identification was employed for Gaussian models, while the parameters of the other basis functions were calculated through closed formulas.

We tested the effectiveness of the several methods on the PhysioNet PTB diagnostic ECG database (561 subjects, 10 s each, 12 leads). Trigonometric and B-spline models proved to be the most effective in following the details of the morphology (PRD: $0.51\% \pm 0.62\%$ *and* $0.99\% \pm 0.96\%$*, respectively, on lead V1 at C=21), possibly as they form an orthogonal basis for the specific signal. This property is not shared by Bézier curves and Gaussian basis functions (PRD:* $2.47\% \pm 2.17\%$ *and* $3.57\% \pm 6.83\%$*).*

1. Introduction

The P wave is the first characteristic waveform found in each beat of an electrocardiographical (ECG) recording. It corresponds to the spread of ionic currents through the atrial musculature (activation or depolarization), after the firing of the sinoatrial (SA) node. The P-wave duration has been commonly employed as a marker of atrial conduction, and its prolongation associated with the remodelling induced by an history of atrial fibrillation (AF). However, a slower propagation is not necessarily linked to paroxysmal episodes of AF. The study of the entire P-wave morphology is therefore gaining momentum, in particular for detecting local conduction disturbances which might then lead to AF, but also for characterizing a larger class of pathologies, *i.e.*, ischemic heart disease and congestive heart failure [1, 2]. Hence, a standardized method for signal-averaged P wave analysis has been called for, especially in the clinical management of elderly patients [3].

On the other hand, the analysis of the P wave presents technical challenges due to the small ECG amplitude and the consequently lower signal to noise (SNR) ratio. Signal-averaged P wave analysis, where consecutive P wave are averaged to decrease the impact of noise, was the first solution suggested to cope with this issue. More recently, techniques based on fitting a mathematical model capable of capturing the main morphological features emerged. The morphological features are derived directly from the model. For example, Censi *et al.* presented a P wave model, based on a linear combination of Gaussian functions [4]. Alternatively, Carlson *et al.* tried to model directly the conduction system, of which the P wave is a sort of "impulse response" [5].

In this methodological work, we compared different models for a morphological description of the P wave, from a signal decomposition perspective. Possible morphological parameters, which can be subsequently derived from the models, were not considered, as they depend on the specific class of patients under analysis.

2. Materials and Methods

2.1. ECG data

The signals used in this study were taken from the PhysioNet PTB Diagnostic ECG Database [6] (sampling frequency: 1000 Hz; resolution: 16-bit). 561 ECG segments, each with duration of 10s, were selected from the twelve conventional leads, at the begining of each recording. After detecting QRS complexes, P waves were located in a 200 ms-long window starting 300 ms before the R waves.

2.2. Signal Decomposition

Let us consider the P wave samples $x(t_i)$, collected in the $(1 \times n)$ vector $\boldsymbol{x}$. Our goal is to model them with $\hat{x}(t_i)$, produced by the linear combination of basis functions $\phi_k(t)$, that is [7]

$$\hat{x}(t_i) = \sum_{k=0}^{N-1} c_k \phi_k(t_i) \quad \text{or} \quad \hat{x} = \boldsymbol{c}^T \boldsymbol{\Phi}, \tag{1}$$

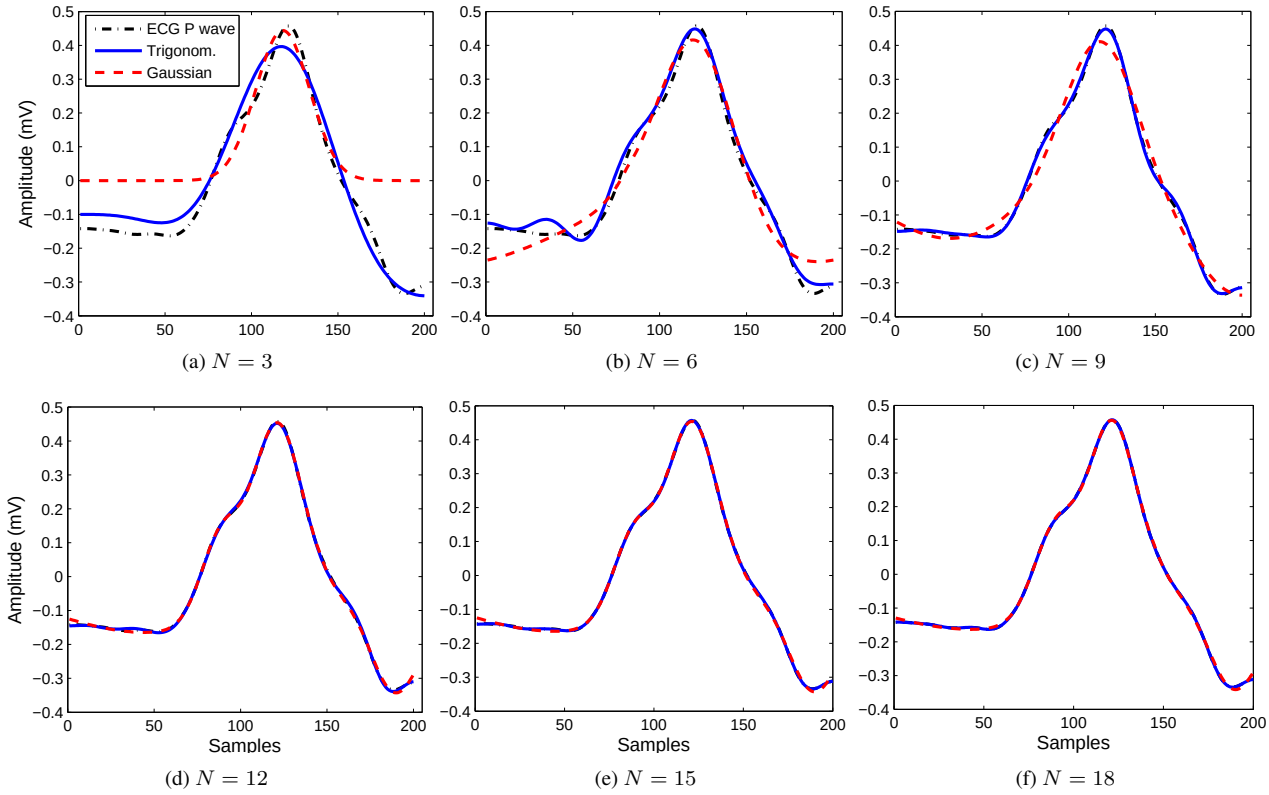

(a) $N = 3$ (b) $N = 6$ (c) $N = 9$

(d) $N = 12$ (e) $N = 15$ (f) $N = 18$

Figure 1. Trigonometric and Gaussian functions-based models for a real P-wave (subject `s0001_re`, lead 2).

where c_k are N scalar coefficients and $\boldsymbol{c}$ their corresponding $(N \times 1)$ vector. $\boldsymbol{\Phi}$ is a $(N \times n)$ matrix containing on each row the basis functions sampled at the instants t_i. The only unknown parameters are the coefficients c_k and they can be obtained by minimizing the energy of the residual signal $\hat{x}(t_i) - x(t_i)$, that is the scalar cost function

$$\begin{aligned} \text{SMSSE}(\boldsymbol{x}|\boldsymbol{c}) &= \left\|\boldsymbol{x}^T - \boldsymbol{\Phi}^T\boldsymbol{c}\right\|_2^2 \\ &= (\boldsymbol{x} - \boldsymbol{c}^T\boldsymbol{\Phi})(\boldsymbol{x}^T - \boldsymbol{\Phi}^T\boldsymbol{c}). \end{aligned}$$

Taking the derivative of $\text{SMSSE}(\boldsymbol{x}|\boldsymbol{c})$ with respect to $\boldsymbol{c}$, and after algebraic manipulations, we get

$$\boldsymbol{c} = (\boldsymbol{\Phi}^T)^+\boldsymbol{x}^T = (\boldsymbol{\Phi}^+)^T\boldsymbol{x}^T = \boldsymbol{\Phi}(\boldsymbol{\Phi}^T\boldsymbol{\Phi})^{-1}\boldsymbol{x}^T \qquad (2)$$

The P wave is a continuous function defined on a compact support $[a, b]$. If the functions $\{\phi_k(t)\}$ are a *complete* set of $\mathbb{L}^2\{[a, b]\}$ then any finite energy signal $x(t)$, defined over $[a, b]$, can be approximated at a selected precision with (1). Moreover, if $\{\phi_k(t)\}$ also form an *orthonormal basis*, the expansion is not redundant and the relative amplitudes of c_k convey information about the relevance of each of the basis functions in the construction of the signal.

In the following several basis functions will be considered: polynomial splines (Bézier and B-spline), trigonometric and Gaussian functions. However the framework can be extended to other functions such as wavelets.

2.2.1. Polynomial Spline Basis Functions

Polynomial splines have been extensively used for curve fitting and interpolation [8]. Among the different types of polynomial splines, Bézier and B-splines satisfy many of the aforementioned properties required for signal modeling. For a finite support signal $x(t)$ defined for $t \in [a, b]$, Bézier basis functions of order p (also known as Bernstein polynomials [8, Ch. 5]) are defined as:

$$\phi_k(t) = \binom{p}{k}\left(\frac{t-a}{b-a}\right)^k\left(\frac{b-t}{b-a}\right)^{p-k}. \qquad (3)$$

Therefore, following (1), the resulting signal's model is

$$\hat{x}(t) = \sum_{k=0}^{N-1} c_k \binom{p}{k}\frac{(t-a)^k(b-t)^{p-k}}{(b-a)^p}. \qquad (4)$$

The Bézier spline in (4) is a polynomial of order $N - 1$. However local control is not achieved by Bézier curves, since the change of the control points (which is fixed) will affect the whole curve shape [9]. B-Spline curves can be used to solve this problem.

Once selected a non-decreasing sequence of real numbers $\{t_j\}_{j=0}^{N+p}$, known as *knots* or *node sequences*, a B-

Table 1. Performances (mean PRD over all P-waves and leads) of the different approximations for different models' orders.

Model	N						
	3	**6**	**9**	**12**	**15**	**18**	**21**
Gaussian	49.98±0.6%	24.9±0.9%	15.3±0.9%	10.02± 1.0%	7.00±0.7%	5.40±0.6%	4.01±0.7%
Bézier	34.66±1.2%	17.76±1.1%	11.06±0.7%	7.62± 0.6%	5.32±0.4%	3.46±0.2%	2.09±0.2%
B-spline	20.18±1.2%	11.74±0.8%	7.58±0.6%	4.77± 0.3%	2.34±0.2%	1.29±0.1%	0.86±0.1%
Trigonom.	22.68±0.6%	10.98±0.4%	5.88±0.3%	3.13± 0.2%	1.64±0.2%	0.91±0.2%	0.58±0.1%

spline of order p is recursively defined as:

$$\phi_j^p(t) = \frac{t - t_j}{t_{j+p-1} - t_j}\phi_j^{p-1}(t) + \frac{t_{j+p} - t}{t_{j+p} - t_{j+1}}\phi_{j+1}^{p-1}(t)$$

where

$$\phi_j^0(t) = \begin{cases} 1 & \text{if } t_j \le t < t_{j+1} \\ 0 & \text{elsewhere} \end{cases}.$$

The function $\phi_j^p(t)$ is identically zero outside the interval $t_j < t < t_{j+p}$ and its supporting interval is $t_j < t < t_{j+1}$. Order p B-splines are linearly independent and the signal $x(t)$ can be modelled as

$$\hat{x}(t) = \sum_{k=0}^{N-1} c_j \phi_j^p(t).$$

The piecewise definition of B-splines and the possibility of selecting the position of the knots make the model highly flexible. They also have other interesting properties, including the fact that their interpolants rapidly converge to the $\mathrm{sinc}(\cdot)$ function, as the degree p increases, and they might degenerate into a Bézier spline. Finally, the local control property is also achieved since B-splines have compact support.

In our simulations, we subdivided the temporal interval where the P-wave was defined, into N identical segments. The knots at the extremes of the interval were repeated, so to have exactly $N - 1 + p$ knots (*e.g.*, $\phi_{N-1}^p(t)$ was supported on $t_{N-1} < t < t_N = \cdots = t_{N-1+p}$).

2.2.2. Sinusoidal (Trigonometric) Functions

P-waves can be approximated also by a linear mixture of sinusoidal basis functions:

$$\hat{x}(t) = \sum_{k=0}^{N-1} c_k \cos(\omega_k t + \psi_k) \tag{5}$$

where c_k, f_k and ψ_k are respectively, the amplitude, frequency and phase of the k-th sinusoid, and $\omega_k = 2\pi f_k$. However using directly a discrete model is more practical for numerical modeling. From the theory of discrete Fourier transform (DCT), it is known that a discrete time signal $x[i]$ of length n can be approximated by a linear mixture of $N \le n$ discrete cosine functions

$$\hat{x}[i] = \frac{1}{n}\sum_{k=0}^{N-1} c_k \cos\left[\omega_k(2i+1)\right] \tag{6}$$

where $\omega_k = k\pi/(2n)$ and $\hat{x}[i] = \hat{x}[t_i]$. This expansion, known as DCT-II, is one of the four common DCT transforms [10, Ch. 8]. Since the set $\{\phi_k[i]\}$ form an orthogonal basis for discrete signals of length n, $\boldsymbol{\Phi}^T\boldsymbol{\Phi} = \boldsymbol{I}/(2n)$. Moreover, the model error $e[i] = x[i] - \hat{x}[i]$ is zero for $N = n$, while for $N < n$ its power is minimized selecting the coefficients c_k as:

$$c_k = \beta_k \textstyle\sum_{i=0}^{n-1} x[i] \cos\left[\omega_k(2i+1)\right] \tag{7}$$

where $\beta_0 = 1$ and $\beta_k = 2$ for $1 \le k \le N-1$.

We should note that the DCT-II provides higher power compaction against sinusoidal basis function [10, Ch. 8]. Finally, comparing equation (5) with equation (1), $\phi_k(t) = \cos(\omega_k t + \psi_k)$ which depends on the two additional parameters ω_k and ψ_k. However, in the DCT-II expansion, ω_k was evenly selected between 0 and the sampling frequency (only the lowest frequencies are then retained in the model) and the fitting of the phase ψ_k implicitly becomes a linear problem due to trigonometric identities.

2.2.3. Gaussian Basis Functions

Each P wave can also be modeled by a superposition of Gaussian kernels with different amplitudes and widths, centered at specific points in time [4]. According to (1),

$$\hat{x}(t) = \sum_{k=0}^{N-1} c_k \phi_k(t) = \sum_{k=0}^{N-1} c_k \exp\left[-\frac{(t-t_k)^2}{2b_k^2}\right]. \tag{8}$$

However, each Gaussian kernel in (8) depends nonlinearly on two additional parameters: t_k and b_k. Unfortunately, there is no analytical formula to identify these parameters from observed data, as the problem is associated with the solution of an over-determined system of nonlinear equations. Levenberg-Marquardt nonlinear least squares were employed to minimize directly the cost function $\mathrm{SMSSE}(\boldsymbol{x}|\boldsymbol{c})$ and fitting the model in equation (8).

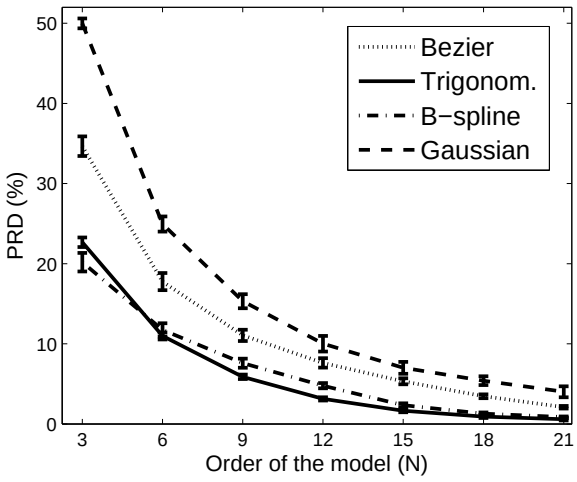

Figure 2. Mean PRD, averaged over any P-wave and lead, versus the order of the model.

The higher computational costs, due to the lack of a closed form solution, make the Gaussian expansion less practical for an automated fitting.

A comparison of trigonometric and Gaussian functions-based models for a P-wave obtained from a real ECG is shown in Fig. (1) at different model orders N.

3. Results

The percentage root-mean-square difference (PRD), a classical compression efficiency measure, was employed to compare the performances of the different models. PRD was calculated as:

$$\mathrm{PRD} = 100\sqrt{\frac{\sum_{\mathrm{i}=1}^{\mathrm{N}}\left(\hat{\mathrm{x}}[\mathrm{t_i}]-\mathrm{x}[\mathrm{t_i}]\right)^2}{\sum_{\mathrm{i}=1}^{\mathrm{N}}\mathrm{x}[\mathrm{t_i}]^2}}, \qquad (9)$$

where x and $\hat{x}$ are the original and modelled P wave. We term compression ratio the value: $r = N/n$.

The mean results are summarized in Fig. 2, for a number of free parameters N ranging from 3 to 21, and Table 1. As a reference, each original P-wave was 200 samples long, so r ranged from 1.5% to 10.5%. Trigonometric models displayed the minimum mean PRD. Together with B-spline models, they proved to be the most effective in following the details of the morphology (PRD: $0.51 \pm 0.62\%$ and $0.99 \pm 0.96\%$, respectively, on lead V1 at C=21), a possible explanation being that they form an orthogonal basis. This property is not shared by Bézier curves and Gaussian basis functions (PRD: $2.47 \pm 2.17\%$ and $3.57 \pm 6.83\%$). Correspondingly, the number of free parameters necessary to have a mean $PRD < 5\%$ in lead II, increased: C=10 for trigonometric, 11 for B-splines, 15 for Bézier polynomials and 18 for Gaussian functions.

4. Discussion and Conclusion

Different approaches for morphological modeling of P waves, based on signal decomposition, were compared. The different methods were able to follow the morphology in details. This suggests that, in practice, they could be successfully employed for amplitude assessment as well as model-based filtering (given the fact that the P-wave frequency content is mainly located in the low frequencies). In applications where the compactness of the model is an advantage, trigonometric model and B-spline were found to be preferable.

References

[1] Platonov PG. P-wave morphology: Underlying mechanisms and clinical implications. Ann Noninvasive Electrocardiol 2012;17:161–169.

[2] Herreros A, Lázaro EB, Johansson R, Carlson J, Perán JR, Olsson B. Analysis of changes in the beat-to-beat P-wave morphology using clustering techniques. Biomed Signal Process Control 2009;4:309 – 316.

[3] Michelucci A, Bagliani G, Colella A, Pieragnoli P, Porciani MC, Gensini G, Padeletti L. P-wave assessment: state of the art update. Cardiac Electrophysiol Rev 2002;6:215220.

[4] Censi F, Calcagnini G, Ricci C, Ricci R, Santini M, Grammatico A, Bartolini P. P-wave morphology assessment by a Gaussian functions-based model in atrial fibrillation patients. IEEE Trans Biomed Eng 2007;54:663–672.

[5] Carlson J, Johansson R, Olsson B. Classification of electrocardiographic P-wave morphology. IEEE Trans Biomed Eng 2001;48:401–405.

[6] Goldberger AL, Amaral LAN, Glass L, Hausdorff JM, Ivanov PC, Mark RG, Mietus JE, Moody GB, Peng CK, Stanley HE. PhysioBank, PhysioToolkit, and PhysioNet components of a new research resource for complex physiologic signals. Circulation 2000;101:e215–e220.

[7] Kheirati Roonizi E, Sameni R. Morphological modeling of cardiac signals based on signal decomposition. Comput Biol Med 2013;43:1453–1461.

[8] Cohen E, Riesenfeld RF, Elber G (eds.). Geometric Modeling with Splines: An Introduction. A K Peters/CRC Press, Natick (MA), 2001.

[9] Diercks P. Curve and surface fitting with splines. Oxford: Oxford University Press, 1995.

[10] Oppenheim A, Schafer R, Buck J. Discrete-time signal processing. Prentice Hall, Upper Saddle River (NJ), 1999.

Address for correspondence:

Ebadollah Kheirati Roonizi
Dipartimento di Informatica
Università degli Studi di Milano
Via Bramante 65, Crema, 26013, Italy
Email: ebadollah.kheirati@unimi.it